Label-free sensors based on perylenediimide-doped polystyrene distributed feedback lasers

María A. Díaz-García*[a], Marta Morales-Vidal[a], José M. Villalvilla[a], Pedro G. Boj[b], José A. Quintana[b], Aritz Retolaza[c], Santos Merino[c]

[a]Dept. Física Aplicada and Instituto Universitario de Materiales de Alicante (IUMA), Universidad de Alicante (UA), Alicante 03080, Spain; [b]Dept. Óptica, Farmacología y Anatomía, and IUMA, UA, Alicante 03080, Spain; [c]Micro and Nano Fabrication Unit, IK4-Tekniker, Eibar 20600, Spain

ABSTRACT

Distributed feedback (DFB) laser sensors with active films consisting of a highly efficient and photostable perylenediimide dye (perylene orange, PDI-O) dispersed in polysytrene (PS), used as passive matrix, are reported. PDI-doped-PS DFB lasers show an excellent operational durability under ambient conditions, superior to those of previously reported DFBs used for sensing purposes. Their bulk refractive index sensing capabilities, under exposure to liquids of different refractive index, have been determined from changes in their emission wavelength. The role of the active film thickness on both, the laser and the sensing performance, has been explored. The use of a thick active film (850 nm) allows obtaining the lowest possible threshold and highest operational lifetime for this type of device although the sensor sensitivity is lower than that achievable with a thin film (160 nm). It is also shown that the inclusion of a high refractive index TiO_2 layer on top of the sensor structure allows improving the sensor sensitivity by around two times.

Keywords: sensors, label-free, organics, lasers, distributed feedback, photostability.

1. INTRODUCTION

Label-free refractive index sensors are ideal devices for highly sensitive and possibly specific non-intrusive sensing with great potential in a variety of applications such as drug discovery, biological research, diagnostic tests, food safety, and environmental monitoring.[1] The second-order solid-state organic distributed feedback (DFB) laser,[2,3] consisting of a waveguide film which includes a relief grating, has emerged as a very promising label-free sensor, as the vertical surface emission enables a contactless excitation and detection, where the biosensor chip is isolated from the rest of the system.[4,5] The DFB sensor generates its own light, so it does not require coupling to an external tunable light source, which constitutes an important advantage with respect to passive optical resonator sensors such as those based on photonic crystals,[6,7] whispering gallery modes[8] or surface plasmon resonances.[9]

The emission wavelength (λ_{DFB}) of a DFB laser is close to the wavelength at which the cavity resonates (λ_{Bragg}), which is determined by the grating period (Λ), the diffraction order (m) and the effective refractive index (n_{eff}), according to the Bragg condition:

$$m\,\lambda_{Bragg} = 2\,n_{eff}\,\Lambda \qquad (1)$$

The n_{eff} parameter depends on the refractive index (n) of film, substrate and cover layer, and on film thickness (h). The DFB structure provides both, the feedback mechanism and the out-coupling for the laser. For sensing purposes, it is important that the laser operates in the second-order (m = 2 in Eq. 1), as to obtain the maximum laser output in a direction perpendicular to the active film (by first-order diffraction). The deposition of superstrates of different refractive index on top of the DFB device results in changes in the laser wavelength, due to changes in n_{eff}, which constitutes the operational principle of the sensor. The bulk refractive index sensitivity (Sb) is defined as the derivative of the lasing wavelength shift, ($\Delta\lambda$), with respect to the n value of the substance deposited onto of the device, that is $d(\Delta\lambda)/dn$.

Organic Field-Effect Transistors XIV; and Organic Sensors and Bioelectronics VIII, edited by Iain McCulloch, Oana D. Jurchescu, Ioannis Kymissis, Ruth Shinar, Luisa Torsi, Proc. of SPIE Vol. 9568, 956823

DFB sensors reported in the literature are based on different types of active materials, such as organic semiconducting molecules[10] or polymers;[11] or laser dyes dispersed in passive polymers, used as matrixes.[4,5,12,13] To date, DFB sensors based on perylenediimide (PDI) laser dyes have not been reported. A relevant feature of PDIs is the simultaneous combination, when dispersed in thermosplastic polymers such as polystyrene (PS), of an excellent photostability under operation in ambient conditions and a relatively low threshold.[14,15] DFB lasers based on PS doped with the PDI derivative called perylene orange (PDI-O, see chemical structure in Figure 1) have shown thresholds as low as 3 kW/cm^2 and device lifetimes up to 10^5 pump pulses, considerably better than those of DFB sensors based on other materials. Another prominent feature of PDI-doped PS materials is their thermal and chemical stability, which enables grating imprinting by thermal nanoimprint lithography (thermal-NIL) directly onto the active film and consequently in a very simple and economical way.[16]

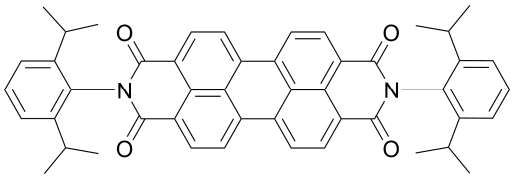

Figure 1. Chemical structure of perylene orange (PDI-O).

A typical strategy to increase a DFB sensor sensitivity is to use a very thin active film,[13,17] although this leads to an increase of its threshold[18] and consequently to a decrease in the operational lifetime.[14,19] Such detriment of the laser performance is due to the decrease of waveguide mode confinement, film absorption and emitted light intensity.[18] Therefore, finding a way to improve the sensitivity while keeping simultaneously a low DFB threshold and high operational lifetime is of great interest. Both laser parameters are important to develop inexpensive organic laser sensors compatible with compact pump sources.[20]Another reported strategy to increase the DFB sensor sensitivity consists in depositing high refractive index layers on top of the active film.[12,13,17]

In this work we have fabricated DFB lasers based on PDI-O-doped PS active films and demonstrate their bulk refractive index sensing capability. The role of the active film thickness on the laser parameters (emission wavelength, threshold and operational durability) and on the sensor sensitivity is studied by exploring devices with two different film thickness (h), 160 and 850 nm. The analysis of the thickness influence on the device threshold is accomplished in combination with the amplified spontaneous emission (ASE) characterization of films without resonators. We have also fabricated and characterize sensor DFB devices including a high refractive index TiO_2 layer on top of the structure.

2. EXPERIMENTAL SECTION

The basic DFB sensor prepared consists of a PDI-O-doped PS film deposited over a one dimensional (1D) DFB grating engraved on a transparent fused silica substrate, see Figure 2. Its refractive index capability has been tested by depositing different liquid superstrates: distilled water, aqueous solutions of glycerin and pure glycerin. We also prepared some devices which include an additional 30 nm-thick TiO_2 layer on top of the active layer. For ASE studies, samples consisting of active films deposited over bare fused silica (without gratings) were used.

The DFB gratings were prepared by thermal nanoimprint lithography (NIL) and subsequent etching, as described elsewhere.[18] The overall size of the grating was (2 mm × 2 mm) and its period and depth were Λ = 376 nm and d = 60 nm, respectively. The TiO_2 layers were prepared by sputtering. The active films were deposited by spin-coating toluene solutions containing PS, as passive matrix, and 1.0 wt% (with respect to PS) of PDI-O on top of the grating (or over the bare substrates for ASE studies). After deposition, active films were heated at 90º C for 120 min to eliminate the residual solvent. The percentage of PS with respect to the solvent was adjusted in order to obtain h values of 160 or 850 nm, depending on the device. Film thickness was determined by the fringe pattern of the absorption spectrum, measured by a Jasco V-650 UV-VIS spectrophotometer.

DFB emission characterization was performed under excitation with a pulsed Nd:YAG (YAG-yttrium aluminium garnet) laser (5.5 ns, 10 Hz) operating at 532 nm. The pump beam over the sample (elliptical with a minor axis of 1.1 mm) was

incident at an angle of around 20° with respect to the normal to the film plane. Light was collected with a fiber spectrometer, in a direction perpendicular to the sample surface. The resolution in determining the spectral peak wavelength and linewidth is 0.07 nm and 0.13 nm, respectively. Excitation and light emission collection is done through the substrate, with the sample placed horizontally with respect to the optical table to facilitate the deposition of liquid superstrates (see Figure 2). This geometry, which requires the use of a transparent substrate, avoids disturbing the analyte with the pump beam. ASE characterization was performed with the same excitation source used for the DFB studies, but here the excitation beam over the sample is a stripe of dimensions 3.50 mm by 0.53 mm and is incident upon it in a perpendicular direction. The stripe was placed right up to the edge of the film, from where PL emission was collected with an Ocean Optics USB2000-UV-VIS fiber spectrometer with a resolution in determining the emission linewidth of 1.3 nm. The precision in measuring the emission wavelength was around half of this value.

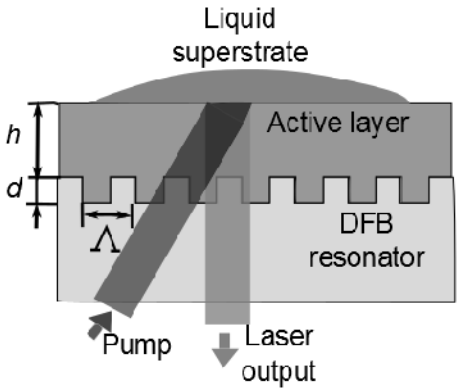

Figure 2. Scheme of DFB laser sensor consisting of a PDI-O-doped PS film of thickness *h* deposited over a fused silica substrate with a one-dimensional DFB grating of period Λ and depth *d*. The superstrate is a drop of liquid solution. The excitation and collection geometry used for device operation is also shown.

3. RESULTS AND DISCUSSION

3.1. Basic DFB sensors.

We have prepared DFB sensors with film thickness of 160 nm and 850 nm. The election of h = 160 nm aimed to have the lowest possible h value for this device. Note that in order to have lasing from this type of waveguide based devices, it is required that h is large enough as to enable the propagation of the fundamental transverse electric (TE_0) waveguide mode. In other words, h should be larger than the so called cut-off thickness for the TE_0 mode, which for the present structure is 149 nm.[21] On the other hand, the film with h = 850 nm supports two waveguide modes, TE_0 and TE_1 (the cut-off thickness for the propagation of the TE_1 mode is 600 nm). The motivation of using such thick h value was to make a DFB device operating at a wavelength associated to the TE_1 mode, instead of at the TE_0 one. This would presumably allow obtaining a higher sensitivity because the slope of the n_{eff} curve (and therefore that of λ_{Bragg}, see Eq. 1) versus h for the TE_1 mode is larger than that of the TE_0 one. [21]

The sensing capability of these devices is illustrated in Figure 3, which shows the shift experienced by the laser emission wavelength upon deposition of a water droplet, with respect to air ($\Delta\lambda_{A\text{-}W}$). It is seen that the largest $\Delta\lambda_{A\text{-}W}$ value is obtained with the device based on the thin film ($\Delta\lambda_{A\text{-}W}$ = 4.2 nm), although as discussed below its laser threshold is rather high because mode confinement is poor. The laser based on the thick film shows a much smaller $\Delta\lambda_{A\text{-}W}$ value for the TE_0 mode ($\Delta\lambda_{A\text{-}W}$ = 0.6 nm). Interestingly this shift is around two times larger for the TE_1 mode ($\Delta\lambda_{A\text{-}W}$ = 1.3 nm). Despite the lower sensitivity of this device in comparison to the thin film, its advantage is that its laser threshold is much lower. In order to determine the *Sb* value of these devices, they were exposed to other liquids besides water (water solutions of glycerin at various rates, and pure glycerin) as to obtain a curve for $\Delta\lambda$ versus n. Then, *Sb* was calculated near the refractive index value of 1.33 (the biological range). Results are shown in Table 1. The value obtained for the thin film (*Sb* = 32 nm/RIU, see Figure 2), is comparable to those reported for other single-layer waveguide DFB sensors

(*Sb* = 20 nm/RIU at n = 1.33),[4,10] which have demonstrated their capability to detect biomolecules.[4,22] This indicates that our PDI-O-based DFB sensors have sufficient sensitivity to be used for biomolecule detection.

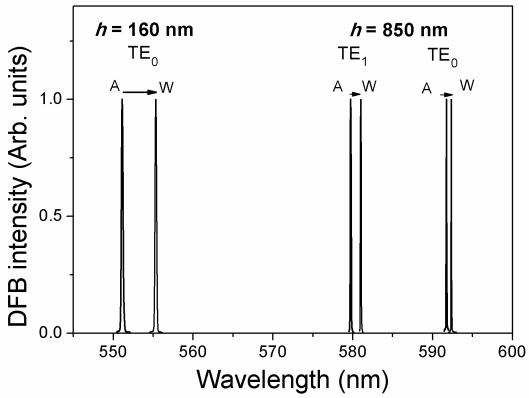

Figure 3. Laser spectra (output DFB intensity, versus emission wavelength) in air (A) and upon water deposition (W) of PDI-O-doped PS DFB sensors with two different film thickness: h = 160 nm, showing a single DFB peak associated to TE_0 mode; and h = 850 nm, showing two DFB peaks associated to TE_0 and TE_1 mode. The wavelength shift between air and water is $\Delta\lambda_{A\text{-}W}$ (TE_0)= 4.2 nm (device with h = 160 nm); and $\Delta\lambda_{A\text{-}W}$ (TE_1) = 1.3 nm and $\Delta\lambda_{A\text{-}W}$ (TE_0) = 0.6 nm (device with h = 850 nm).

The DFB emission wavelength (λ_{DFB}) and threshold ($I_{th\text{-}DFB}$) of these devices are listed in Table 1. For the laser based on the thick film, which shows two peaks, data for each of them are provided. ASE data (wavelength, λ_{ASE}, and threshold, $I_{th\text{-}ASE}$) for films of the same characteristics, but deposited over substrates without gratings are also included in the table. The reason for studying also the ASE properties is that λ_{ASE} is practically independent on h, while λ_{DFB} is very sensitive to it. So ASE allows making a proper analysis of the role of the waveguide mode confinement on the threshold.[21] Importantly, $I_{th\text{-}ASE}$ for the thick film is only 6 kW/cm^2, in contrast to the high value obtained with the thin film (120 kW/cm^2). This is due to the lower absorption of the latter, and therefore PL intensity, as well as to a poorer confinement of the waveguide mode.[21] A consequence of the large ASE threshold of the thin film is that its photostability half-life is reduced, since the film requires a higher pumping intensity for operation. For instance, the ASE photostability half-life of the thin film is one order of magnitude lower than that of the thick film, which is as high as 2×10^5 pump pulses, under excitation two times above $I_{th\text{-}ASE}$.

Table 1. Sensitivity and laser parameters of PDI-O-doped PS DFB sensors and ASE parameters of similar films deposited over substrates without gratings: active film thickness (h); laser wavelength (λ_{DFB}) and threshold ($I_{th\text{-}DFB}$) of the laser exposed to air; shift in λ_{DFB} upon water deposition over the sensor surface ($\Delta\lambda_{A\text{-}W}$); sensor sensitivity in the biological range (Sb); ASE wavelength (λ_{ASE}) and threshold ($I_{th\text{-}ASE}$).

h (nm)	$\Delta\lambda_{A\text{-}W}$ (nm)	Sb at n = 1.33 (nm/RIU)	λ_{ASE} (nm)	$I_{th\text{-}ASE}$ (kW/cm^2)	λ_{DFB} (nm)	I_{thDFB} (kW/cm^2)
160	4.2 (TE_0)	32 (TE_0)	577.9	120	551.1 (TE_0)	210 (TE_0)
850	0.6 (TE_0) 1.3 (TE_1)	3.2 (TE_0) 7.6 (TE_1)	580.8	6	591.7 (TE_0) 579.7 (TE_1)	20 (TE_0) 3 (TE_1)

With regards to the DFB parameters, λ_{DFB} is highly dependent on h (this parameter affects n_{eff}). The $I_{th\text{-}DFB}$ value for the thin film, which shows a single peak associated to the TE_0 mode, is rather large (210 kW/cm^2) mainly because λ_{DFB} is far from the wavelength of maximum gain (given by λ_{ASE}), but it is also because $I_{th\text{-}ASE}$ is large. On the other hand, for the

device based on the thick film, the $I_{th\text{-}DFB}$ value for the peak associated to the TE_0 mode is only 20 kW/cm^2, despite λ_{DFB} is far from λ_{ASE}. It is remarkable that $I_{th\text{-}DFB}$ for the peak associated with the TE_1 mode, whose λ_{DFB} is very close to λ_{ASE}, is only 3 kW/cm^2. As for the DFB operational lifetime, results are in accordance with previously discussed ASE photostability performance: the device based on a thick film shows a half-life of around 10^4 pump pulses (under excitation two times above $I_{th\text{-}DFB}$), being this value one order of magnitude smaller than that of the laser with the thick film.

3.2. DFB sensors with top TiO_2 layer.

The effect on the sensing performance of depositing a thin (30 nm-thick) layer of TiO_2 was investigated in the two devices described in section 3.1. First of all, the λ_{DFB} value of the sensor exposed to air appears at a significantly different wavelength than the one of the device without TiO_2. Note that for TiO_2, n = 2.4 (at λ = 580 nm). Particularly, for the sensor with h = 160 nm, λ_{DFB} appears at a value 10 nm above the one obtained without TiO_2 layer (see Figure 4). Upon water deposition, the shift in the emission wavelength is $\Delta\lambda_{A\text{-}W}$ = 10.2 nm and the sensitivity in the biological range (determined as in previous section) is *Sb* = 60 nm/RIU. This *Sb* value is around two times larger than that of the device without TiO_2, and is comparable to that reported by other authors with laser sensors with top TiO_2 layers based on other materials.[13] For this device, the DFB spectrum consisted of a single peak associated with the TE_0 mode, except in the case of glycerin exposure which showed an additional peak corresponding to the TE_1 mode.

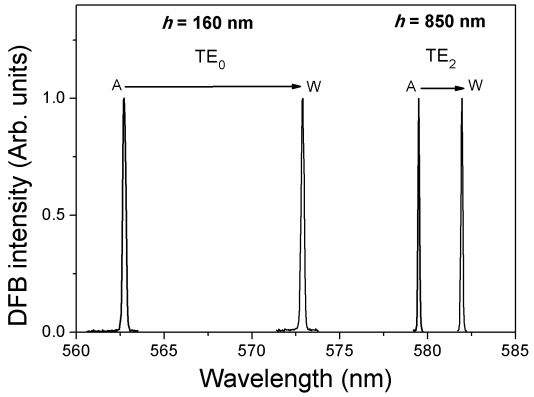

Figure 4. Laser spectra (output DFB intensity, versus emission wavelength) in air (A) and upon water deposition (W) of two PDI-O-doped PS DFB sensors (with h = 160 nm and h = 850 nm), including a layer of TiO_2 on top of the active. Data shown correspond to peaks associated, respectively, with the TE_0 mode and the TE_2 mode. The wavelength shift between air and water is $\Delta\lambda_{A\text{-}W}$ (TE_0) = 10.2 nm (device with h = 160 nm) and $\Delta\lambda_{A\text{-}W}$ (TE_2) = 2.5 nm (device with h = 850 nm).

In the case of the device with h = 850 nm and the TiO_2 layer, the DFB spectrum consists of several peaks, associated to different waveguide modes. For instance, two peaks associated to TE_1 and TE_2 modes, when the sensor is exposed to air; three peaks, related to TE_1, TE_2 and TE_3 upon water deposition, etc. The existence of several peaks complicates the sensing analysis. Only the peak associated to the TE_2 mode allows sensing ($\Delta\lambda_{A\text{-}W}$ = 2.5 nm and *Sb* = 16 nm/RIU, see Figure 4) in the range of refractive indexes studied here because it is the only one appearing in all cases (in air, water, etc..). As for the device based on a thin active film, the *Sb* is also in this case larger than that of the device without TiO_2 layer. Finally, with regards to the laser thresholds of these devices including a top TiO_2 layer, they were found to be around two times larger than those without TiO_2. This can be attributed to the presence of higher order modes, although a detailed interpretation of this issue is not an obvious task, since it depends on various parameters as already discussed.

4. CONCLUSIONS

The use of DFB lasers based on highly photostable perylenediimide-based active films for bulk refractive index sensing has been demonstrated. The sensor sensitivity, *Sb*, has been determined in the biological range (at n = 1.33) from changes in the laser emission wavelength upon exposure to liquids of different refractive index. The role of the active

film thickness, h, on the sensing and the laser performance has been analyzed. A high sensitivity of $Sb \sim 32$ nm/RIU is obtained with a DFB sensor based on a very thin film ($h = 160$ nm), operating at a laser threshold of 200 kW/cm^2 with an operational durability of around 10^4 pump pulses (under a pump intensity two times above threshold) at a wavelength associated to the fundamental transverse electric (TE_0) waveguide mode. The increase of h up to around 850 nm allows improving both, the laser threshold and the operational durability, by two orders of magnitude. In this case, a higher sensitivity is achieved when the sensor operates at the wavelength corresponding to the first-order TE_1 mode, instead of at the TE_0 one. It has also been shown that the inclusion of a high refractive index TiO_2 layer on top of the sensor structure improves the sensitivity by around two times.

ACKNOWLEDGEMENTS

This work was supported by the Spanish Government (MINECO) and the European Community (FEDER) through grant no. MAT-2011–28167-C02. M.M-V. has been partly supported by a MINECO FPI fellowship (no. BES-2009-020747).

REFERENCES

[1] Fan, X., White, I.M., Shopova, S.I., Zhu, H., Suter, J.D. and Sun, Y., "Sensitive optical biosensors for unlabeled targets: A review," Anal. Chim. Acta 620, 8-26 (2008).
[2] Chénais, S. and Forget, S., "Recent advances in solid-state organic lasers," Polym. Int. 61, 390-406 (2012).
[3] Grivas, C. and Pollnau, M., "Organic solid-state integrated amplifiers and lasers," Laser Photonics Rev. 6 (4), 419-462 (2012).
[4] Lu, M., Choi, S.S., Wagner, C.J., Eden, J.G. and Cunningham, B.T., "Label free biosensor incorporating a replica-molded, vertically emitting distributed feedback laser," Appl. Phys. Lett. 92, 261502 (2008).
[5] Tan, Y., Ge, C., Chu, A., Lu, M., Goldshlag, W., Huang, C.S., Pokhriyal, A., George, S. and Cunningham, B.T., "Plastic-based distributed feedback laser biosensors in microplate format," IEEE Sens. J. 12 (5), 1174-1180 (2012).
[6] Kristensen, M., Krüger, A., Groothoff, N., García-Rupérez, J., Toccafondo, V., García-Castelló, J., Bañuls, M.J., Peransi-Llopis, S. and Maquieira, A., "Photonic crystal biosensor chip for label-free detection of bacteria," Proc. OSA, SWB1 (2011).
[7] Shamah, S.M. and Cunningham, B.T., "Label-free cell-based assays using photonic crystal optical biosensors," Analyst 136, 1090-1102 (2011).
[8] Volmer, F. and Arnold, S., "Whispering-gallery-mode biosensing: label-free detection down to single molecules," Nat. Methods 5 (7), 591-596 (2008).
[9] Koubová, V., Brynda, E., Karasová, L., Škvor, J., Homola, J., Dostálek, J., Tobiška, P. and Rošický, J., "Detection of foodborne pathogens using surface plasmon resonance biosensors," Sens. Actuators B: Chem. 74, 100-105 (2001).
[10] Haughey, A.M., Guilhabert, B., Kanibolotsky, A.L., Skabara, P.J., Burley, G.A., Dawson, M.D. and Laurand, N., "An organic semiconductor laser based on star-shaped truxene-core oligomers for refractive index sensing," Sens. Actuators B: Chem. 185, 132-139 (2013).
[11] Heydari, E., Buller, J., Wischerchoff, E., Laschewsky, A., Döring, S. and Stumpe, J., "Label-free biosensor based on all-polymer DFB laser," Adv. Opt. Mater. 2, 137-141 (2014).
[12] Lu, M., Choi, S.S., Irfan, U. and Cunningham, B.T., "Plastic distributed feedback laser biosensor," Appl. Phys. Lett. 93, 111113 (2008).
[13] Vannahme, C., Leung, M.C., Richter, F., Smith, C.L.C., Hermannsson, P.G. and Kristensen, A., "Nanoimprinted distributed feedback lasers comprising TiO_2 thin films: design guidelines for high performance sensing," Laser Photonics Rev. 7 (6), 1036-1042 (2013).
[14] Navarro-Fuster, V., Calzado, E.M., Boj, P.G., Quintana, J.A., Villalvilla, J.M., Díaz-García, M.A., Trabadelo, V., Juarros, A., Retolaza, A. and Merino, S., "Highly photostable organic distributed feedback laser emitting at 573 nm," Appl. Phys. Lett. 97, 171104 (2010).
[15] Ramírez, M.G., Morales-Vidal, M., Navarro-Fuster, V., Boj, P.G., Quintana, J.A, Villalvilla, J.M., Retolaza, A., Merino, S. and Díaz-García, M.A., "Improved performance of perylenediimide-based lasers," J. Mater. Chem. C 1, 1182-1191(2013).

[16] Ramírez, M.G., Boj, P.G., Navarro-Fuster, V., Vragovic, I., Villalvilla, J.M., Alonso, I., Trabadelo, V., Merino, S. and Díaz-García, M.A., "Efficient organic distributed feedback lasers with imprinted active films," Opt. Express 19 (23), 22443-22454 (2011).
[17] Lu, M., "Label-free biosensor based upon replica-molded vertically emitting distributed feedback laser", Ph. D. Thesis, Graduate College of the University of Illinois, Urbana-Champaign, (2009).
[18] Navarro-Fuster, V., Vragovic, I., Calzado, E.M., Boj, P.G., Quintana, J.A., Villalvilla, J.M., Retolaza, A., Juarros, A., Otaduy, D., Merino, S. and Díaz-García, M.A. "Film thickness and grating depth variation in organic second-order distributed feedback lasers," J. Appl. Phys. 112, 043104 (2012).
[19] Calzado, E.M., Villalvilla, J. M., Boj, P.G., Quintana, J.A., Navarro-Fuster, V., Retolaza, A., Merino, S. and Díaz-García, M.A., "Influence of the excitation area on the thresholds of organic second-order distributed feedback lasers," Appl. Phys. Lett. 101, 223303 (2012).
[20] Tsiminis, G., Wang, Y., Kanibolotsky, A.L., Inigo, A.R., Skabara, P.J., Samuel, I.D.W. and Turnbull, G.A., "Nanoimprinted Organic semiconductor laser pumped by a Light-Emitting Diode," Adv. Mater. 25, 2826-2830 (2013).
[21] Calzado, E.M., Ramírez, M.G., Boj, P.G., Díaz-García, M.A., "Thickness dependence of amplified spontaneous emission in low-absorbing organic waveguides," Appl. Opt. 51, 3287-3293 (2012).
[22] Haughey, A.M., Guilhabert, B., Kanibolotsky, A.L., Skabara, P.J., Dawson, M.D., Burley, G.A., Laurand, N., "An oligofluorene truxene based distributed feedback laser for biosensing applications," Biosens. Bioelectron. 54, 679-686 (2014).